ELSEVIER

Polymer 42 (2001) 4527–4532

polymer

www.elsevier.nl/locate/polymer

Long-term service performance of polymeric materials from short-term tests: prediction of the stress shift factor from a minimum of data

Ali E. Akinay, Witold Brostow*

Departments of Materials Science and Chemistry, University of North Texas, Denton, TX 76203-5310, USA

Received 10 July 2000; received in revised form 17 October 2000; accepted 13 November 2000

Abstract

We use the time–stress correspondence (TSC) principle and consider creep compliance D data for a polymer liquid crystal (PLC). A master compliance plot is created from two stress σ levels only; the lower stress level is the reference while the other set is shifted on the logarithmic time axis. The master plot so created is quite close to that constructed after a significant amount of experimentation at several σ levels. A formula for stress shift factor a_σ obtained by one of us is applied for the prediction of a_σ values for the other σ levels. Again, a low σ level is used as the reference while D values for two higher σ levels are used in calculations. The predicted a_σ values agree with the experimental ones within the limits of the experimental accuracy. Very close values of the Doolittle constant B are obtained from different subsets of minimum amounts of results and also from the full set of experiments for nine stress levels. The accuracy of the results is affected by the stress range covered (a wider range gives better results) but not by the amount of data used. © 2001 Published by Elsevier Science Ltd.

Keywords: Polymer service performance; Time–stress correspondence; Stress shift factor

1. Introduction

We consider viscoelasticity, which is the time dependence of mechanical properties of polymers, as an opportunity for life and long-term service performance prediction [1–4]. In this paper, we aim to prove that we can predict long-term properties accurately from a small number of results — instead of the usual quite extensive experimentation involving a number of variables. Starting with the classical work of Ferry [5,6] there have been numerous studies involving the time–temperature correspondence (TTC) and also the frequency–temperature correspondence related to TTC [1,2,4,7–9]. Tschoegl and co-workers have extended the TTC principle by inclusion of hydrostatic pressure [10–15]. In 1948, O'Shaughnessy demonstrated experimentally the existence of time–stress correspondence (TSC) [16]. In the next half a century, however, much less attention was paid to TSC than to TTC. A small number of attempts to apply TSC were described by Goldman [8].

Thus, our primary objective is to reduce the amount of experimental data from short-term experiments needed for the long-term prediction of performance of viscoelastic materials. Our secondary objective is to draw attention to the usefulness of TSC. To achieve our aims, in the next section we discuss the foundations of the correspondence principles. In Section 3, we discuss general formulae which make possible quantitative calculations based on the principles. It is on this basis that we then discuss ways of significantly cutting down on the experimentation and yet making reliable predictions.

2. Foundations of the correspondence principles

To arrive at the basis for the principles, we make two important assumptions. First, the response of the material to an external mechanical force is treated as a collective rather than individual reaction of polymer chain segments. This has been assumed by Kubat and co-workers [17–19] to explain experimental stress relaxation curves. Indeed, his model based on this assumption predicts the experimental results well [17–20]. Moreover, a direct conformation of the collective behavior has been provided by molecular dynamics computer simulations [21,22]. The other assumption we make consists of adopting the concept of the chain relaxation capability (CRC) [1–4]. CRC can be defined as the amount of external energy dissipated by relaxation in a unit of time per unit weight of the polymer.

We are concerned with the basic types of response of a polymeric material to deformation. Therefore, we need to list important processes which take place in such a material

* Corresponding author.
E-mail address: brostow@unt.edu (W. Brostow).

0032-3861/01/$ - see front matter © 2001 Published by Elsevier Science Ltd.
PII: S0032-3861(00)00835-1

when a mechanical force is applied to it: transmission of energy across the chain; transmission of energy to the neighboring chains where segmental motions as well as entanglements play a role; conformational rearrangements of the chains; elastic energy storage resulting from bond stretching and angle changes; and phase transformation toughening first observed for polymers by Kim and Robertson [23] and later analyzed by Karger-Kocsis [24]. All these processes inside the polymeric material require free volume v^f. The larger v^f creates a larger maneuvering ability of the chains and thus higher CRC.

The effects of v^f on thermo-physical and mechanical properties have been studied extensively, respectively, by Flory [25,26] and Ferry [6]. Free volume can be defined as

$$v^f = v - v^* \tag{1}$$

where v is the total specific volume (for instance in $cm^3\ g^{-1}$) and v^* the characteristic (incompressible or hard-core) volume corresponding to a very high pressure and zero thermodynamic temperature. The reduced volume $\tilde{v}$ and the other reduced parameters are defined as follows:

$$\tilde{v} = v/v^*; \qquad \tilde{T} = T/T^*; \qquad \tilde{P} = P/P^* \tag{2}$$

where T and P are the thermodynamic temperature and pressure; T^* and P^* the characteristic (hard-core) parameters for a given material. The former is related to the strength of interactions in the material. P^* is a complicated function of the intermolecular interactions and of the material structure represented by the binary radial distribution function $g(R)$ [27].

The connection between v^f and the correspondence principles has been discussed extensively, notably by Ferry [6] and Goldman [8]. High v^f at elevated temperatures enables the processes listed above — the constituents of CRC — to occur faster than at low temperatures. This is how we can determine long-term behavior at low temperatures from short-term tests at high temperatures. Morphology of the polymer is reflected in v^f, and Schwarzl and Staverman argued in 1952 that there is a connection between TTC and morphology [28]. More importantly, as argued in particular by one of us [29], *any* method of varying v^f provides a potential for long-term prediction. Temperature variation just happens to be the method used most often.

The use of Eq. (1) requires the knowledge of v^*. The relation between $(T/T^*)^{3/2}$ and v^f has been derived and tested for several polymer liquids by Litt [30–32]. Similarly, T^* and P^* can only be evaluated by the application of a specific equation of state. Good results have been obtained repeatedly [4,9,19,31,33,35] by using the Hartmann equation [36,37], which is valid for both polymer melts and solids:

$$\tilde{P}\tilde{v}^5 = \tilde{T}^{3/2} - \ln \tilde{v} \tag{3}$$

3. Time–temperature and time–stress correspondence principles

TTC can be used as the basis of determination of a mechanical property of interest as a function of time at several temperatures. One can then create a master curve extending over several decades of time for a chosen temperature T_{ref}. To give just one example, the master curve of tensile creep compliance for a polymer liquid crystal (PLC) extends over 16 decades of time [4]. Temperature shift factor a_T (or $\ln a_T$) is used to shift individual curves until they coalesce into the master curve.

Predictions based on TTC require a formula for the temperature dependence of the shift factor, $a_T(T)$. Starting from the Doolittle equation connecting the viscosity η to v^f [38], one of us has derived such a general formula [1,2]

$$\ln a_T = A + B/(\tilde{v} - 1) \tag{4}$$

Here A and B are material constants and B appears in the Doolittle equation. The reduced volume $\tilde{v}$ is related to temperature T via an equation of state. The pioneering Williams–Landel–Ferry (WLF) equation for a_T of 1955 [5] is a special case of Eq. (4). As stressed by Ferry [6], the WLF equation is usable only between the glass transition temperature T_g and $T_g + 50$ K. Cases are known when the WLF equation was applied outside of the range prescribed by Ferry, and then bad results erroneously blamed on inapplicability of the TTC principle. Eq. (4) does not have such limitations since any changes in the volumetric behavior of the material are reflected in the equation of state (EOS) — provided that the EOS is accurate. This is why we use the Hartmann Equation (3) as the EOS. Good results have been obtained using Eqs. (3) and (4) together for several kinds of polymers, including polyethylenes, polyurethanes and also a PLC [4] which forms four phases in its service temperature range [39]. We note that two distinct sets of v^*, T^* and P^* have been created in Ref. [39] for our material, one set for the solid and the other for the liquid state. The first-order phase change affects the characteristic parameters significantly. As expected, T^* is lower in the molten state since intersegmental distances are larger. However, the characteristic parameters for the liquid state cover the range from the melting to the clearing temperatures including the transition from the smectic E to the smectic B phase. Thus, in such a range, approaches such as ours are expected to work.

Given the natural connection between time t and frequency ω in dynamic oscillatory (e.g. sinusoidal) experiments, we have temperature–frequency correspondence as a subsidiary to TTC [8]. Thus, master curves in terms of frequency have been created for instance for tan δ of high density polyethylene (HDPE) pre-drawn to various values of the draw ratio λ [9]. To provide predictive capabilities in this case also, Eq. (4) was generalized to the form

$$\ln a_T = 1/(a + c\lambda) + B/(\tilde{v} - 1) \tag{5}$$

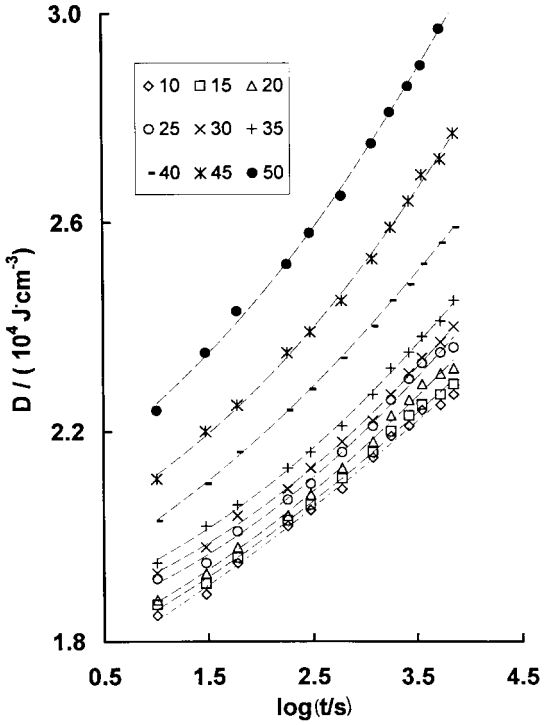

Fig. 1. Experimental creep compliance for PET/0.6PHB as a function of log time between 10 and 50 J cm^{-3} stress levels with 5 J cm^{-3} intervals at $T = 20°C$.

where clearly $1/A$ in Eq. (4) is now replaced by $a + c\lambda$. Here a and c are material constants independent of the degree of orientation and of temperature. The denominator of the first term in Eq. (5) represents a measure of the orientation caused by drawing. Eq. (5) also predicts the values within the limits of the experimental accuracy.

It is clear that the stress level σ affects free volume and thus CRC. We have already briefly noted the work of O'Shaughnessy [16]; he reported that compliance values of rayon from creep experiments for different stress levels will coalesce into a single master curve when plotted against time or a function of time. However, a reliable formula for the stress shift factor a_σ as a function of stress σ to predict long-term behavior of polymers was not available. Now one of us has derived such a formula using the CRC concept; details of the derivation are provided elsewhere [29]. The resulting equation is

$$\ln a_\sigma = \ln[v(\sigma)/v_{\text{ref}}] + B[(\tilde{v} - 1)^{-1} - (\tilde{v}_{\text{ref}} - 1)^{-1}] + C(\sigma - \sigma_{\text{ref}}) \quad (6)$$

where $v_{\text{ref}} = v(\sigma_{\text{ref}}, T_{\text{ref}})$, B is the Doolittle constant as before, while C is a constant representing the effects of varying stress on the chain conformations and structure of the material. Positive values of C mean that the viscosity η increases under stress. Thus, experiments at several stress levels can be used for prediction of long-term behavior in a similar way as experiments at several temperatures are used.

In Sections 4 and 5, respectively, we explain the criteria for the material selection for our calculations and discuss the validity of Eq. (6).

4. Material selection

As already mentioned above, there is a PLC which forms four phases in its service temperature range [39]. It is longitudinal, that is it has the LC sequences in the main chain and oriented along the backbone [40,41]. The PLC has been thoroughly characterized before [39,42,43]. The chemical formula is PET/0.6PHB; PET, poly(ethylene terephthalate); PHB, *p*-hydroxybenzoic acid (LC); 0.6, the mole fraction of PHB. In another paper [44] we report extensive creep compliance data for this material. We shall see whether a small subset of these data will be sufficient for predictive purposes.

5. Application of the TSC principle and of Eq. (6) to a large set of data

The time dependence of creep compliance D as a function of logarithmic time at the room temperature of 20°C has been investigated at several stress σ values [44]. Fig. 1 shows D versus log time t curves at different σ levels in the range from 10 to 50 J cm^{-3}. As reported by Kubat and Maksimov [19], the σ level range for our polymer covers non-linear viscoelasticity.

We quote briefly the results reported in Ref. [44] for a large set of experimental data since they will serve as the standard for comparison with results obtained from our new procedure. We have applied the TSC to the results shown in Fig. 1. We have chosen $\sigma_{\text{ref}} = 10$ J cm^{-3} as the reference stress level for which $a_\sigma = 1$ by definition. Then, we have shifted the results for all other stress levels building a single master curve shown in Fig. 2. The respective shifting distance is the stress shift factor a_σ defined as follows:

$$D(t, T_{\text{ref}}, \sigma) = D(ta_\sigma, T, \sigma) \quad (7)$$

The validity of Eq. (6) has also been investigated. The characteristic parameters $v^* = 0.682$ cm^3 g^{-1}, $T^* = 1400$ K and $P^* = 3850$ J cm^{-3} for our PLC have been determined using the Hartmann Equation (3) from the experimental PVT data [34]. These parameters and Eq. (5) have been used to compute $\tilde{v}$ and v values for the corresponding stress levels. The results have then been used in Eq. (6). B and C values obtained by fitting the data in Fig. 2 are equal to 5.10 and -0.52, respectively. A good agreement between the experimental and calculated a_σ has been achieved and is shown in Fig. 3. The continuous line in that figure has been obtained using Eq. (6) and can be compared with all the experimental results (asterisks). The dotted line will be discussed later. Therefore, we conclude that varying stress can serve equally well for the prediction of long-term behavior from short-term tests as varying the temperature. As briefly noted

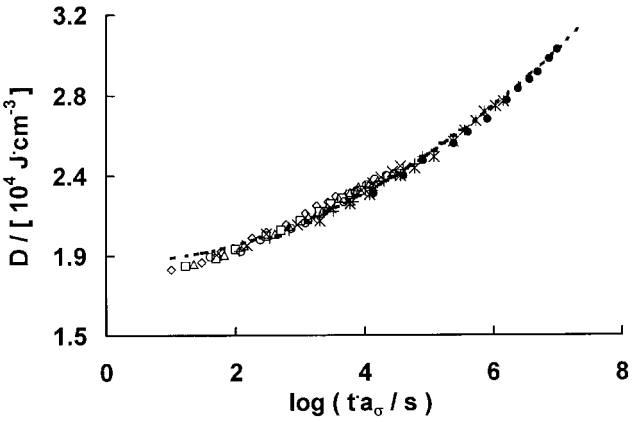

Fig. 2. The master curve for PET/0.6PHB of creep compliance as a function of $\log ta_\sigma/s$ for $\sigma_{ref} = 10\ J\ cm^{-3}$. Points are experimental values and symbols are the same as in Fig. 1. The discontinuous curve is fitted to the equation $y = 0.0231x^2 + 1.89$.

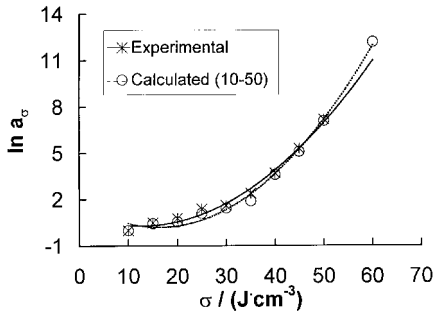

Fig. 3. The logarithmic stress shift factor $a_\sigma(\sigma)$ for the PET/0.6PHB. Continuous line is fitted to experimental values (asterisks) by using Eq. (6) in conjunction with Eq. (3); the resulting values are $B = 5.10$ and $C = -0.52$. Open circles are those calculated from three stress level results: $\sigma_{ref} = 10\ J\ cm^{-3}$, and two other higher stress (45 and 50 J cm^{-3}) levels. The discontinuous line is fitted to the open circles; in this case the constants of Eq. (6) are $B = 5.15$ and $C = -0.54$.

above, TTC is used much more often than TSC, but there is no fundamental reason for choosing one over the other.

6. A new approach for creating master curves from data for two stress levels only

We shall now develop a way to evaluate long-term properties accurately on the basis of a small amount of experimental data — instead of the usual basis of extensive experimentation.

We have taken from Fig. 2 the entire set of master plot data and represented this set by a simple two-term equation in which $y = D$ and $x = \log(ta_\sigma/s)$. We have evaluated the parameters in the equation by a least-squares procedure with the result $y = 0.0231x^2 + 1.89$. The discontinuous line in Fig. 2 represents this equation.

We have then performed a similar operation for the set of compliance data including only two stress levels. Thus, Fig. 4 has been obtained by using the set of data for the lowest ($\sigma = 10\ J\ cm^{-3}$) and the highest ($\sigma = 50\ J\ cm^{-3}$) stress levels. The resulting equation reads $y = 0.0235x^2 + 1.89$ and is represented by the discontinuous line in Fig. 4. We see that the equation of this form serves well both for the full set and the small subset, one parameter has not changed at all, while the change in the value of the other parameter is not large.

Given these results for the extreme stress levels, one expects that using intermediate stress levels should render similar results. Calculations of the same kind have also been performed using other pairs of stress levels. Thus, compliance D values for 15, 20 or 25 J cm^{-3} were used as the lower data set while 45, 50 or 35 J cm^{-3} results were taken for the higher D set. Indeed, the parameters of the two-term equation for each such pair are close to those obtained for the full set of experimental data. This proves the feasibility of performing predictions from results for two stress levels only. Thus, we now need an algorithm for calculating the stress shift factor a_σ with sufficient accuracy.

We have defined the necessary algorithm as follows. We take two sets of experimental data for two stress levels only from Fig. 1. Label the lower stress level 1 and the higher level 2. By using a least-squares procedure we calculate the parameters b and c of the two-term equation for each set. Thus, we get

$$y_1 = b_1x^2 + c_1 \tag{8a}$$

$$y_2 = b_2x^2 + c_2 \tag{8b}$$

As before, y is a value of the creep compliance D corresponding to a specific value of $x = \log t$.

As can be seen in Fig. 1, the data sets for low stress values have low slopes and an increase in σ produces an increase of the average slope of the set of data. Given the parameters in Eq. (8a), we shift set 2 towards higher logarithmic time values so that the lowest experimental point of that set lies on the extrapolated curve of set 1. We call this process σ_1 extrapolation and the intersection point x_1.

A similar procedure is performed by using set 2 represented by Eq. (8b). This time, however, the shifting is done so that the lowest point of set 1 appears on the downwards

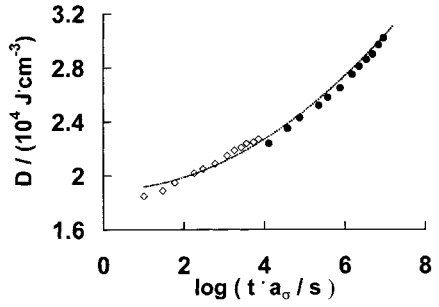

Fig. 4. The master curve for PET/0.6PHB created by using only 10 and 50 J cm^{-3} stress levels creep compliance results as explained in the text. The discontinuous curve is fitted to equation $y = 0.0235x^2 + 1.89$.

Table 1
The comparisons between some of the experimental and calculated $a_{\sigma 1+2}$ values from using two stress levels D results

σ_1 (J cm^{-3})	σ_2 (J cm^{-3})	$a_{\sigma 1+2}$ Experimental	$a_{\sigma 1+2}$ Calculated	% (±) Error
10	50	4.11	4.14	0.73
10	45	3.30	3.31	0.30
10	40	2.60	2.52	3.08
10	35	2.10	2.02	3.81
15	50	4.08	4.06	0.49
15	45	2.80	2.72	2.86
15	40	2.30	2.24	2.61
20	50	3.50	3.60	2.86
20	45	2.80	2.90	3.57
25	50	3.36	3.30	1.79
25	45	2.60	2.50	3.85

extrapolation of set 2 performed with Eq. (8b). The location of the point so defined is called x_2; since set 2 has the higher slope, $x_2 < x_1$.

The average $D(\log t)$ slope increases gradually between the low stress level set 1 and the high stress level set 2. We need to capture that increase. We use the simple arithmetic mean to calculate the location at which set 2 should begin after shifting:

$$a_{\sigma 1+2} = (x_1 + x_2)/2 \tag{9}$$

We shall verify below whether such a simple assumption will be sufficient for obtaining accurate results. At this point the assumption is at least plausible; we have already seen from numerical values of the parameters b_i and c_i for the extreme values $\sigma = 10$ J cm^{-3} and $\sigma = 50$ J cm^{-3} that the slope changes are not dramatic.

We are now ready to create a master curve from compliance results from two stress levels only. We take the lower stress level as σ_{ref}. We shift the higher stress level results by $a_{\sigma 1+2}$ calculated from Eq. (9). The master curve so obtained is that represented by the dotted line in Fig. 4. Comparing it with Fig. 2, we find that it corresponds well to the master curve obtained from the total set of results.

Needless to say, we do not rely on visual comparisons. We have applied the same algorithm to other pairs of stress levels. Each time the lower σ level was used as the reference while the higher set was shifted on the logarithmic time axis so as to create a new master curve according to Eq. (7). The resulting values of the stress shift factors $a_{\sigma 1+2}$ calculated from Eq. (9) are listed in Table 1 for 11 pairs of sets of data.

Assuming the experimental values of $a_{\sigma 1+2}$ at which the higher level points begin to be correct, we have computed the error for each calculated value. The results are listed in the last column of Table 1. As expected, the larger the distance $\sigma_2 - \sigma_1$, the smaller the error. Thus the accuracy of our procedure increases with the size of the stress interval between set 1 and set 2; experiments should be conducted accordingly. Much more importantly, we have succeeded in our main objective of creating the master curve on the basis of the results for the two stress levels only.

7. Prediction of a_σ from three stress levels

Clearly, two sets of experimental data constitute the minimum. Consider now a case when we have avoided extensive experimentation but have at our disposal results for *three* stress levels. It is possible to calculate a_σ values for all σ levels by using Eq. (6) with three constant stress D test results. Again, we find it convenient to define the lowest σ level as the reference. Then, B and C constants of Eq. (6) are calculated by using the middle and highest stress level sets. By taking 10, 45 and 50 J cm^{-3} levels, we obtain $B = 5.15$ and $C = -0.54$. We see that these values are quite close to those quoted in Section 5 obtained from nine stress levels. Open circles in Fig. 3 represent a_σ values obtained using these constants. Thus, using compliance values for three stress levels, nearly the same results are achieved as those for the set of nine levels. We recall that the experimental results are represented by asterisks while the continuous curve has been obtained from Eq. (6).

Similar stress shift factors and master curves are also obtained by using other sets of constant stress level D results. For brevity we include here one more case. We now take the data for 25 J cm^{-3} as σ_{ref}. Then, the same types of calculation as before are performed, taking again as the two upper levels 45 and 50 J cm^{-3}. Eq. (6) now gives us $B = 4.58$ and $C = -0.50$. We see that the C value is still quite close to that obtained from the full set of data while the Doolittle constant B is now lower than that from the full set and from the previous calculation. However, in that earlier calculation we had the stress interval from 10 to 50 J cm^{-3} while we now have only the range from 25 to 50 J cm^{-3}. Once again we find that the amount of data used is *not* crucial but the stress range covered does affect the quality of results. Fig. 5 is the analog of Fig. 3 for the 25–50 J cm^{-3} range. The circles and the dotted line going through them are further from the experiment (asterisks) and from Eq. (6) continuous line than was the case in Fig. 3. However, the outcome for even this narrow range provides satisfactory results for most purposes.

In conclusion, a reliable prediction of service performance of polymers can be achieved on the basis of a

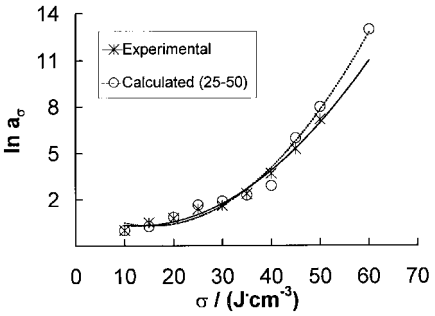

Fig. 5. The logarithmic stress shift factor $a_\sigma(\sigma)$ for the PET/0.6PHB. The continuous line is fitted to experimental values (asterisks) by using Eq. (6) in conjunction with Eq. (3). Open circles are those calculated from three stress level results: $\sigma_{ref} = 25$ J cm^{-3}, and two other higher stress (45 and 50 J cm^{-3}) levels. The discontinuous line is fitted to the open circles after the constants of Eq. (6) $B = 4.58$ and $C = -0.50$ have been calculated.

small number of results of short-term tests. We have found that the use of experimental results from two or three stress levels provides comparable results to the use of nine stress levels.

Acknowledgements

One of us (A.E.A.) would like to thank TUBITAK-NATO, Ankara, for financial support. Partial support has also been provided by the State of Texas Advanced Research Program (Grant No. 003594-0075-1999) and by the Robert A. Welch Foundation (Grant No. B-1203). Discussions with Dr Anatoly Goldman, Alcoa CSI, Crawfordsville, Indiana, and with Dr Bruce Hartmann and Jeffry J. Fedderly, Naval Surface Warfare Center, West Bethesda, Maryland, on the free volume–mechanical properties connection are acknowledged as well. Useful publications on the free volume–temperature relationship supplied by Prof. Morton Litt, Case Western Reserve University, Cleveland, Ohio, are appreciated. Constructive comments of referees have been taken into account and are also appreciated.

References

[1] Brostow W. Mater Chem Phys 1985;13:47.
[2] Brostow W. In: Brostow W, Corneliussen RD, editors. Failure of plastics. Munich/Vienna/New York: Hanser, 1986 [chap. 10].
[3] Brostow W, Kubat J, Kubat MJ. Mechanical properties. In: Mark JE, editor. Physical properties of polymers handbook. Woodbury, NY: American Institute of Physics, 1996 [chap. 23].
[4] Brostow W, D'Souza NA, Kubat J, Maksimov RD. J Chem Phys 1999;110:9706.
[5] Williams ML, Landel RF, Ferry JD. J Am Chem Soc 1955;17:3701.
[6] Ferry JD. Viscoelastic properties of polymers. 3rd ed. New York: Wiley, 1980.
[7] Markowitz H. J Polym Sci Symp 1975;50:431.
[8] Goldman AY. Prediction of the deformation properties of polymeric and composite materials. Washington, DC: American Chemical Society, 1994.
[9] Boiko YM, Brostow W, Goldman AY, Ramamurthy AC. Polymer 1995;36:1383.
[10] Sharda SC, Tschoegl NW. Trans Soc Rheol 1976;20:361.
[11] Fillers RW, Tschoegl NW. Trans Soc Rheol 1977;21:51.
[12] Fillers RW, Tschoegl NW. Trans Soc Rheol 1977;2:51.
[13] Moonan WK, Tschoegl NW. Macromolecules 1983;16:55.
[14] Moonan WK, Tschoegl NW. Int J Polym Mater 1984;10:199.
[15] Moonan WK, Tschoegl NW. J Polym Sci Phys 1985;23:623.
[16] O'Shaughnessy MT. Textile Res J 1948;18:263.
[17] Kubat J. Phys Status Solidi B 1982;111:599.
[18] Kubat J, Rigdahl M. Failure of plastics. In: Brostow W, Corneliussen RD, editors. Munich/Vienna/New York: Hanser, 1986 [chap. 4].
[19] Kubat J, Maksimov RD. Creep and stress relaxation. In: Brostow W, editor. Mechanical and thermophysical properties of polymer liquid crystals. London: Chapman & Hall, 1998. p. 407.
[20] Kubat MJ, Jansson FJ, Delin M, Kubat J, Rychwalski RW, Uggla S. J Appl Phys 1992;72:5179.
[21] Brostow W, Kubat J. Phys Rev B 1993;47:7659.
[22] Blonski S, Brostow W, Kubat J. Phys Rev B 1994;49:6494.
[23] Kim J, Robertson JE. J Mater Sci 1992;27:3000.
[24] Karger-Kocsis J. Polym Engng Sci 1996;36:203.
[25] Flory PJ. J Am Chem Soc 1965;87:1833.
[26] Flory PJ. Faraday Soc Discuss 1970;49:7.
[27] Brostow W, Szymanski W. J Rheol 1986;30:877.
[28] Schwarzl F, Staverman AJ. J Appl Phys 1952;23:838.
[29] Brostow W. Mater Res Innovat 2001;3:347.
[30] Litt MH. Trans Soc Rheol 1976;20:47.
[31] Litt MH. Free volume and its relationship to zero shear melt viscosity: a new correlation. In: Meier DJ, editor. Molecular basis of transitions and relaxations. New York: Gordon and Breach Science, 1978. p. 311.
[32] Litt MH. J Rheol 1986;30:853.
[33] Brostow W, Duffy JV, Lee GF, Madejczyk K. Macromolecules 1991;24:479.
[34] Berry JM, Brostow W, Hess M, Jacobs EG. Polymer 1998;39:4081.
[35] Mano J, Sousa RA, Reis RL, Cunha AM, Bevis MJ. Preprint from the University of Minho, Guimaraes, 2000.
[36] Hartmann B, Haque MA. J Appl Phys 1985;58:2831.
[37] Hartmann B, Haque MA. J Appl Polym Sci 1985;30:1553.
[38] Doolittle AK. J Appl Phys 1951;22:1741.
[39] Brostow W, Hess M, Lopez BL. Macromolecules 1994;27:2262.
[40] Brostow W. Polymer 1990;31:979.
[41] Brostow W. Polymer liquid crystals. In: Mark JE, editor. Physical properties of polymers handbook. Woodbury, NY: American Institute of Physics, 1996 [chap. 33].
[42] Brostow W, Hess M, Lopez BL, Sterzynski T. Polymer 1996;37:1551.
[43] Brostow W, Sterzynski T, Triouleyre S. Polymer 1996;37:1561.
[44] Akinay AE, Brostow W, Maksimov RM. Polym Engng Sci 2001;41 [in press].